We are IntechOpen, the world's leading publisher of Open Access books Built by scientists, for scientists

6,900
Open access books available

185,000
International authors and editors

200M
Downloads

Our authors are among the

154
Countries delivered to

TOP 1%
most cited scientists

12.2%
Contributors from top 500 universities



WEB OF SCIENCE™

Selection of our books indexed in the Book Citation Index in Web of Science™ Core Collection (BKCI)

Interested in publishing with us?
Contact book.department@intechopen.com

Numbers displayed above are based on latest data collected.
For more information visit www.intechopen.com



2

Diagnostic Imaging of the Pituitary and Parasellar Region

Joanna Bladowska and Marek Sąsiadek
Department of General Radiology, Interventional Radiology and Neuroradiology
Wroclaw Medical University
Poland

1. Introduction

Pituitary (*hypophysis*), the secreting gland located in the sella turcica, has fascinated the scientists since ages. In 1543 the Belgian scientist Andreas Vesalius described the anatomy of pituitary gland for the first time. He believed that pituitary produces mucus, which is secreted from the brain into the nasal cavity. This is why pituitary was called the mucous gland (*glandula pituitaria; pituita* = *mucus*). Pituitary gland, also called as „master gland" plays the special role in the body. There are plenty of pathological changes with different clinical and radiological appearances of lesions located in sellar and parasellar region. The knowledge of pituitary anatomy and function, as well as of the characteristic changes in size and shape of the pituitary throughout the life and special physiologic conditions, is mandatory for the correct diagnosis and therefore these factors have to be taken into account before assessing pituitary abnormalities.

2. Imaging of pituitary gland

Introduction of imaging modalities, especially magnetic resonance (MR), and of modern methods of neurosurgery and pharmacotherapy revolutionised diagnosis and therapy of pituitary tumours. Currently, MR is the method of choice for imaging of the pituitary gland and the parasellar area. Advanced MR techniques – MR diffusion, MR spectroscopy and MR perfusion – have been increasingly applied (Boxerman et al., 2010; Chernov et al., 2009).

MR imaging protocol of pituitary and sellar region including postoperative studies should consist of unenhanced T1- and T2-weighted images in coronal and sagittal planes (slice thickness 3mm, field of view FOV=16x16). Paramagnetic contrast medium is administrated intravenously at the standard dose of 0.1 ml/kg BM and post-contrast T1-weighted images are taken in coronal and sagittal planes (Bladowska et al., 2004, 2011).

MR examination enables visualization of many anatomic details of pituitary gland, such as: the anterior lobe (adenohypophysis), the posterior lobe (neurohypophysis), pituitary infundibulum, parasellar structures (cavernous sinuses, sphenoid sinus, suprasellar cisterns) and optic chiasm (Bladowska et al., 2004).

The normal pituitary gland shows the homogenous signal intensity, which is isointense compared to the white matter signal on T1-weighted as well as on T2-weighted images

(Fig.1a,b). After contrast administration pituitary gland presents the homogenous strong enhancement (Fig.2a,b).

The posterior lobe of the pituitary demonstrates the characteristic high signal intensity on T1- and T2-weighted images, seen just in front of the sellar dorsum and clearly differentiated from the anterior pituitary lobe. The high signal intensity of the posterior lobe is especially clearly visible on the sagittal planes (Fig. 3a,b) and it is called "posterior pituitary bright spot". This high intensity signal observed in the posterior lobe is believed to be related to intracellular droplets of lipid or lipidlike material in pituicytes (astrocytic glial cells). However, the recent studies using the sequences with fat suppression have not confirmed the presence of fat tissue within the neurohypophysis (Arslan et al., 1999).

Absence of this high intensity signal have been reported in patients with central diabetes insipidus (Fig.4a.b). It has to be stressed that some normal subjects lack this hyperintense

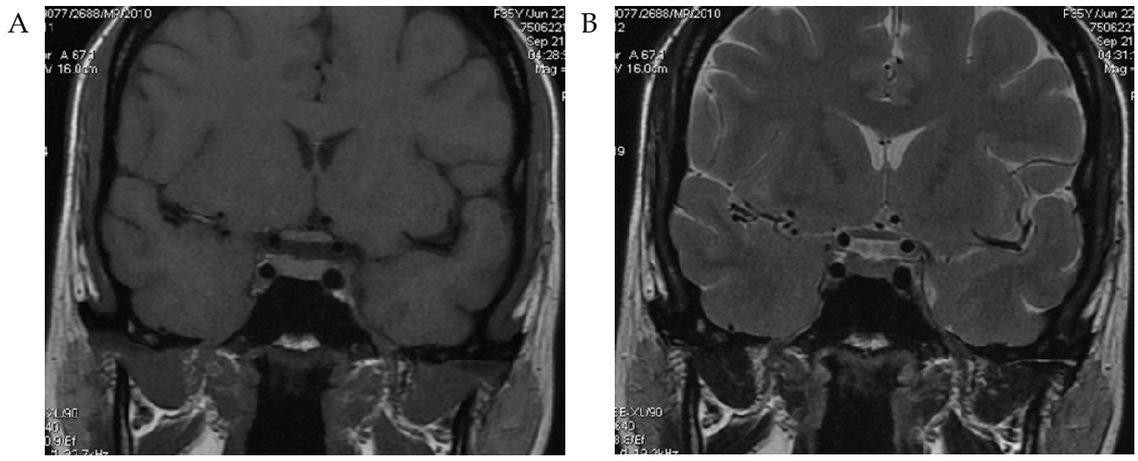


Fig. 1. MR imaging of normal pituitary gland in coronal planes before contrast administration: A. T1-weighted image. B. T2-weighted image.

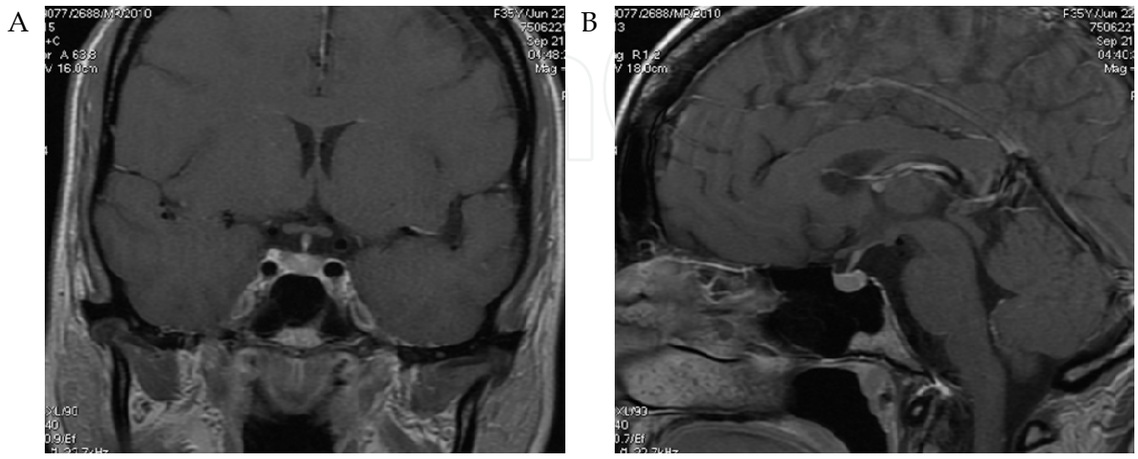


Fig. 2. MR imaging of normal pituitary gland, T1-weighted images after contrast administration: A. Coronal plane. B. Sagittal plane.

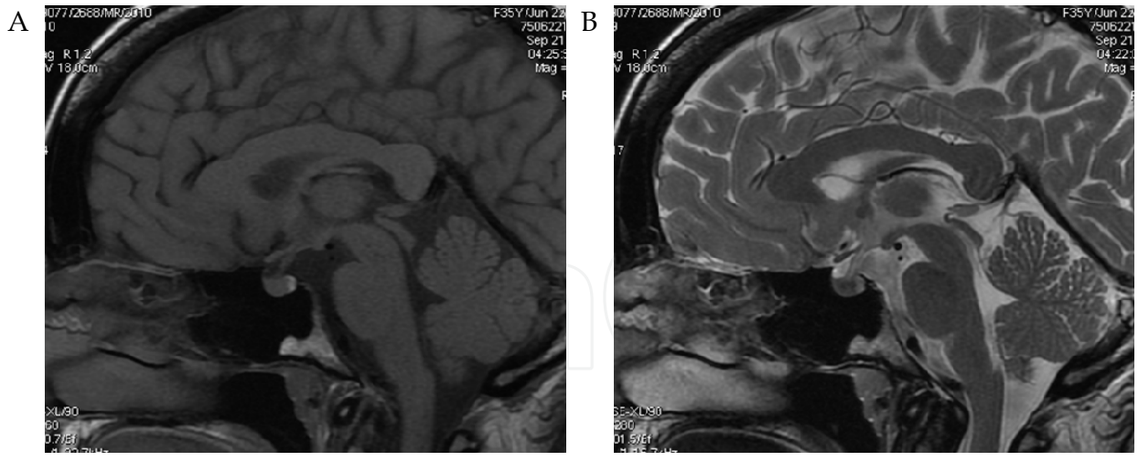


Fig. 3. MR imaging of normal pituitary gland in sagittal planes before contrast administration: A. T1-weighted image. B. T2-weighted image. The high signal intensity of the posterior lobe is clearly visible.

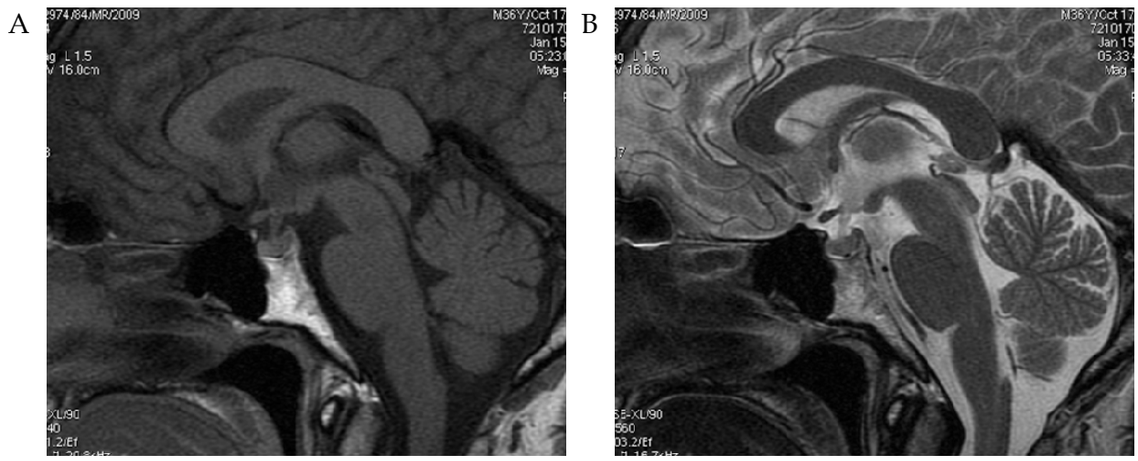


Fig. 4. MR imaging in sagittal planes before contrast administration, a 36-y.o. man with central diabetes insipidus. A. T1-weighted image. B. T2-weighted image. The high signal intensity of the posterior lobe is not visible.

signal of the posterior lobe, therefore its absence cannot be taken as an absolute sign of pituitary disease or dysfunction (Evanson, 2002).

The normal pituitary gland undergoes the characteristic changes in size and shape throughout the life, which have to be taken into account before assessing pituitary abnormalities.

In neonates, the pituitary gland is typically convex and shows a higher signal intensity compared to the brain stem on T1-weighted images (Fig.5). This appearance persists for about 2 months, after which the pituitary will present with a flat superior surface and a signal intensity similar to the signal of the pons, what is typical for the older children.

Throughout childhood, the pituitary reveals a slight but definite growth in all dimensions. The upper surface is flat or mildly concave and the height of the pituitary in the sagittal plane is about 2-6mm (Fig.6a,b), there are no differences between girls and boys.

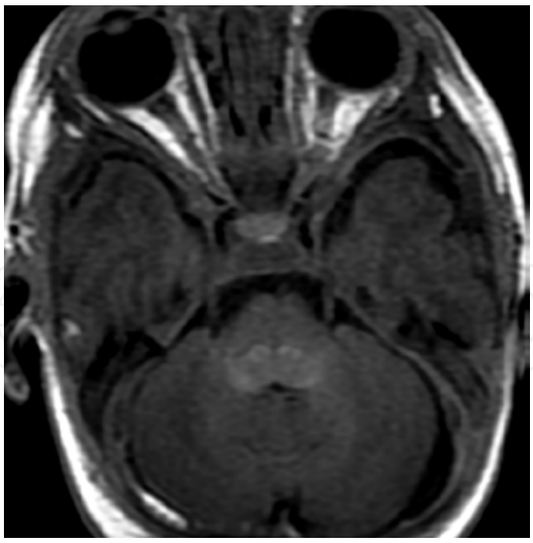


Fig. 5. MR imaging in neonate, T1-weighted image in axial plane. The pituitary gland demonstrates the characteristic high signal intensity.



Fig. 6. MR imaging of normal pituitary gland in 5-y.o. boy, T1-weighted images.: A. Sagittal plane B. Coronal plane after contrast administration.

At puberty the pituitary gland demonstrates the huge changes in size and shape, becoming larger than at any other time of the whole life. In girls the gland can reach the height of 10mm, while in boys it may measure 7-8mm. Furthermore, in pubertal girls the gland can also project above the sella and present with a marked convexity of its superior surface (Elster, 1990, 1993).

Physiologic hypertrophy of the pituitary can be observed during pregnancy, when the gland may increase in weight by 30%-100%. By the third trimester the pituitary usually measures even 10mm of height and shows the typical convex superior surface. It has to be stressed that during pregnancy and the 1st postpartum week, the pituitary gland demonstrates the

high signal intensity on T1-weighted images (Fig.7), like in the neonate period (Bladowska et al., 2004; Elster, 1991, 1993).

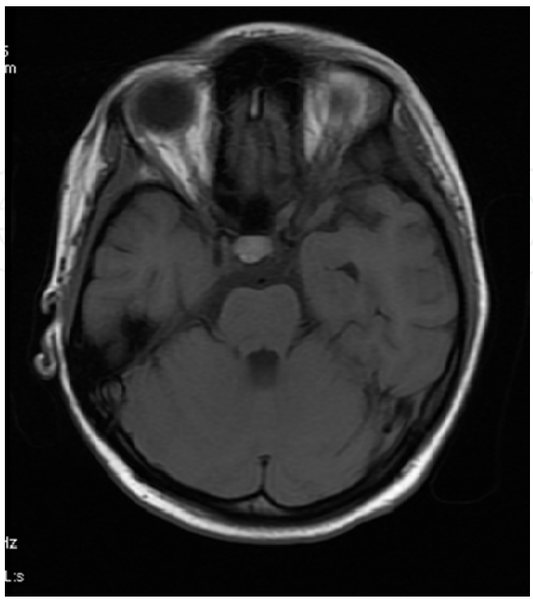


Fig. 7. MR imaging of the pituitary gland in 24-y.o. woman 5 days after delivery, T1-weighted image in axial plane. The pituitary gland demonstrated the characteristic high signal intensity.

From young adulthood until middle age, the pituitary glands of both sexes show usually stable appearance. Beyond age of 50 years, progressive involution of the gland is observed, what is probably related to the decrease in pituitary activity during menopause and andropause period. It has to be emphasized that in about 30% of this population the high signal intensity of the posterior pituitary lobe is not visible, as well as the empty sella syndrome is more commonly noted, but these changes are typical signs of normal aging process (Bladowska et al., 2004; Elster, 1993).

3. Imaging of pituitary adenomas

Pituitary adenomas constitute approximately 10 to 15% of all primary intracranial neoplasms and are the most common causes of pituitary function disorders and field of view deficits. Therefore, early diagnosis and therapy of patients with pituitary tumors are of high importance in clinical practice (Bladowska et al., 2010a).

Pituitary adenomas are the most common pathology encountered in the sellar region. They are usually benign and slow growing tumors, but up to 50% reveal histological evidence of capsule invasion, furthermore less than 0.2% could be malignant, causing local spread into the central nervous system. Pituitary carcinoma is exceedingly rare.

About 70% of pituitary adenomas are diagnosed in patients aged 30-50-y.o., while subjects in age below 20-y.o. constitute only 3 to 7% of all patients with pituitary tumors. Besides, pituitary adenomas are more common in women than in men (Daly et al., 2009).

Pituitary adenomas can be classified on the basis of their size: microadenomas are less than 10mm in diameter and macroadenomas are greater than 10mm. It has to be stressed that the separate term "picoadenomas" should be used for describing the tumors smaller than 3mm, because these lesions are posing special diagnostic problems – it is often impossible to visualize the picoadenomas on MR imaging (Bonneville et al., 2000, 2005).

Furthermore, clinically adenomas are classified depending upon the presence or absence of specific hormonal activity. They are divided into two groups: functioning pituitary adenomas and non-functioning adenomas. Functioning adenomas usually secrete a single hormone causing a well recognised endocrine syndrome like e.g. acromegaly (GH - growth hormone-secreting adenomas).

In MR imaging, on T1-weighted images, about 80-90% of pituitary microadenomas present with lower signal intensity compared to the normal anterior pituitary lobe – they are hypointense. The other cases of microadenomas could be isointense and therefore they will be not visible on T1-weighted images before contrast administration. Pituitary microadenomas can also reveal high signal intensity on T1-weighted images, what may be caused by hemorrhagic transformation of the adenoma and this is a frequent sign in prolactinomas (PRL - prolactine-secreting adenomas). On T2-weighted images, about 1/3 to ½ of microadenomas demonstrate high signal intensity (Fig.8), what is especially helpful in making the correct diagnosis of pituitary pathology. Increased signal intensity on T2-weighted images is noted in over 80% of microprolactinomas. The other types of pituitary microadenomas can present different signal intensity on T2- weighted images, iso or hypointense signal occurs in about 2/3 cases of GH-secreting microadenomas (Bonneville et al., 2005).

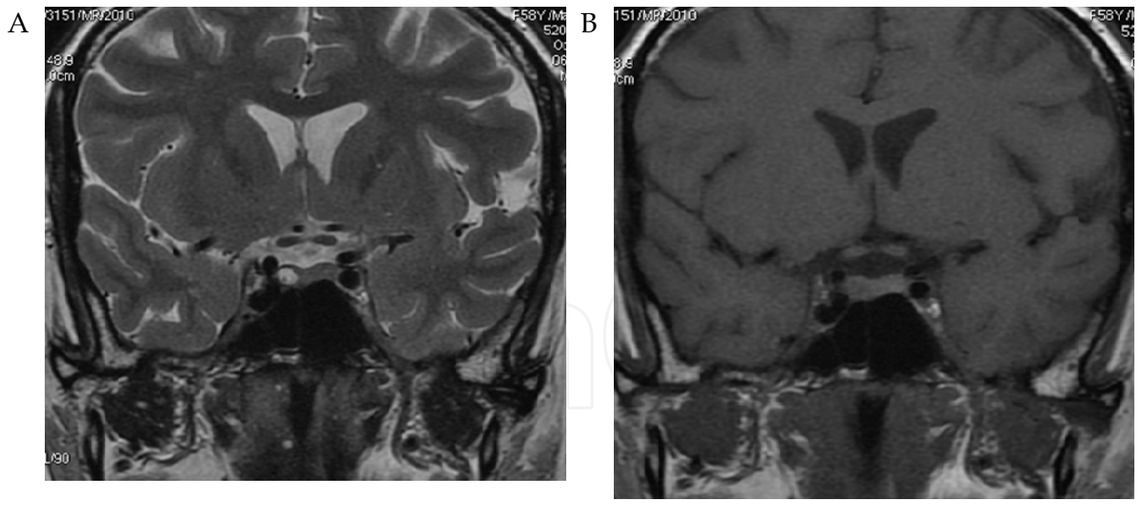


Fig. 8. MR imaging in coronal planes before contrast administration. A. T2-weighted image. B. T1-weighted image. On the right side of the pituitary gland there is a microadenoma, which shows the high signal intensity on T2- weighted image, making the correct diagnosis easy, while it is almost not visible on T1-weighted image.

On the contrast-enhanced T1-weighted images microadenomas can show typically low signal intensity compared to the intense enhancement of the unaffected pituitary gland (Fig.9) (Bladowska et al., 2004).

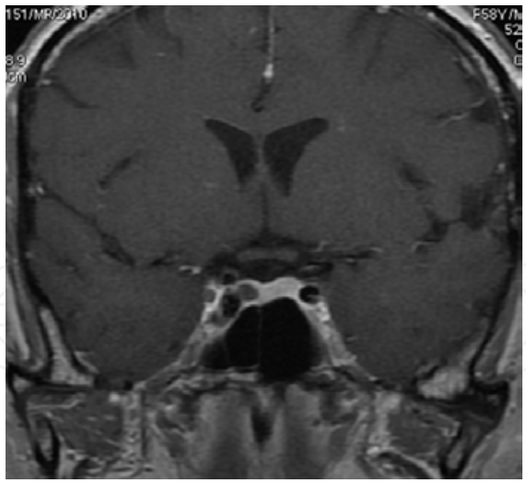


Fig. 9. T1-weighted image in coronal plane after contrast administration. The hypointense microadenoma is visible on the right side of the pituitary gland.

It has to be emphasized, as mentioned above, the contrast-enhancement images may be normal in case of the extremely small tumor (picoadenoma). When the plain MR images are not convincing, other techniques can be also used. The delayed images taken about 30-40 minutes after contrast administration may reveal late enhancement of the microadenoma itself (Bonneville et al., 2005). In our own material of pituitary adenomas we have noticed microadenomas, which show contrast-enhancement just about 10 minutes after injection of contrast (Fig.10a,b).

A B

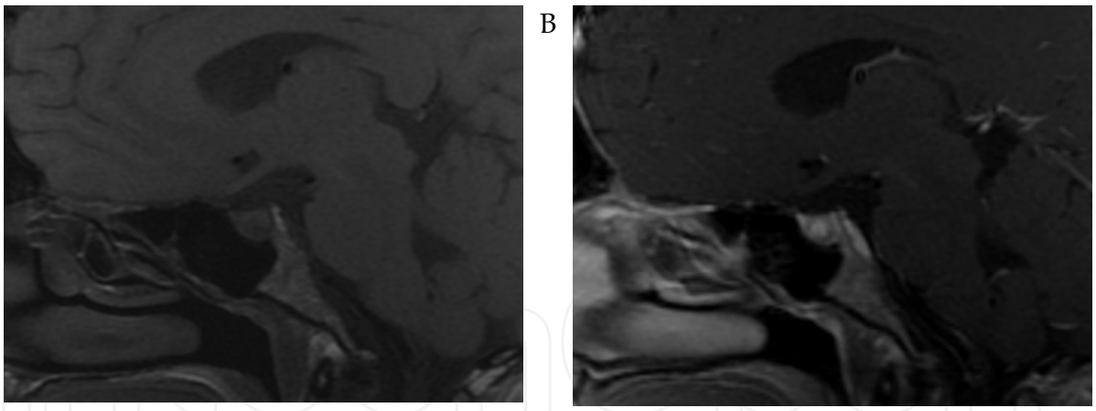


Fig. 10. T1-weighted sagittal images, before (A) and about 10 minutes after contrast administration. On the delayed image the enhancing microadenoma is clearly visible.

The ACTH-secreting microadenomas associated with Cushing's disease tend to be very small (typical feature of picoadenomas) and more often occult on MR imaging (Bonneville et al., 2005; Evanson, 2002). Dynamic imaging can be recommended in the diagnosis of ACTH-secreting microadenomas, when the clinical symptoms are highly suggesting of pituitary pathology, but the plain MR imaging is normal. Dynamic imaging can evidence a lack or a temporary delay of enhancement in the microadenoma compared to the unaffected pituitary gland. However, the delayed images taken at least about 10 minutes after contrast administration seem to be more useful in inconclusive cases.

The diagnosis of macroadenoma in MR imaging is usually simple because of the tumor size over 10mm, making the adenoma clearly visible, even in the computed tomography (CT). However, the other tumors may also be located in the sellar region and they can mimic pituitary adenomas. Therefore, the precise knowledge of the MR appearance of the macroadenomas is of high importance in the clinical practice.

Macroadenomas are usually isointense on T1-weighted images, and after contrast administration they show different enhancement patterns (Fig.11, 12). On T2-weighted images they may be often inhomogenous, with disseminated high intensity areas of cystic degeneration or necrotic regions. About 18% of macroadenomas reveal the cystic components, while about 20% show features of haemorrhage, usually clinically asymptomatic and diagnosed incidentally in MR imaging. Large pituitary adenomas are prone to develop infarction or haemorrhage, because of their tenuous blood supply.

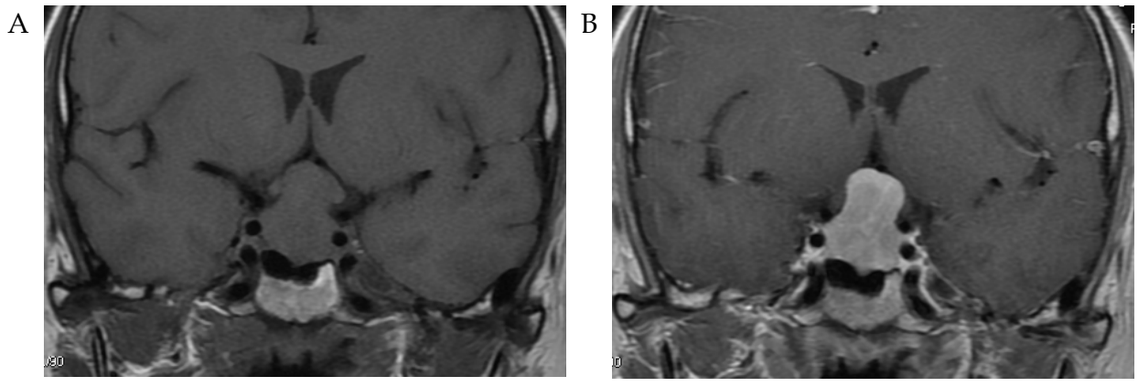


Fig. 11. T1-weighted coronal images before (A) and after contrast administration (B). The sellar-suprasellar macroadenoma shows strong contrast-enhancement. There is evidence of the optic chiasm and the third ventricle compression.

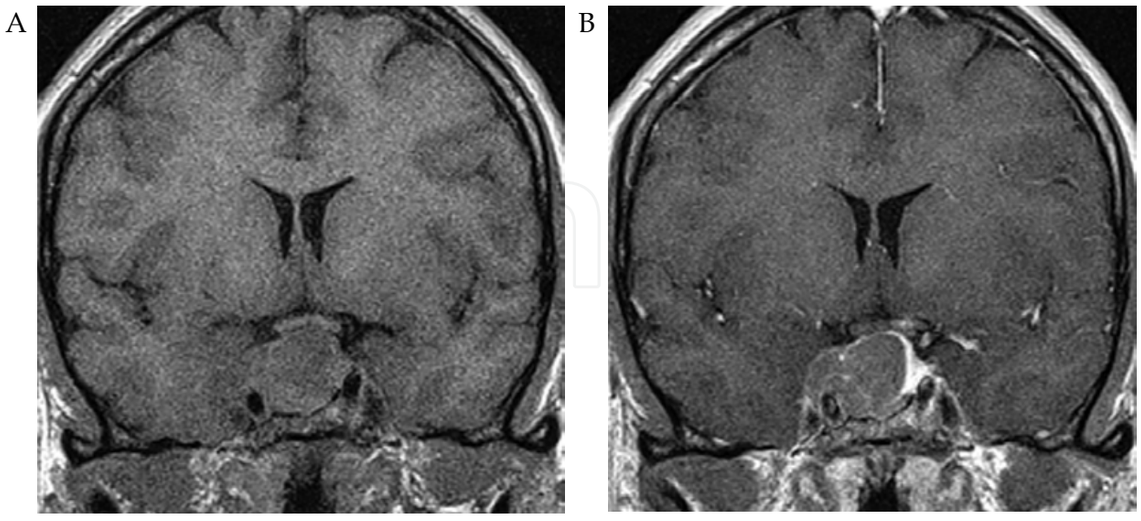


Fig. 12. T1-weighted coronal images before (A) and after contrast administration (B). The macroadenoma does not enhance after contrast injection. The compressed pituitary gland, showing the high signal intensity, is displaced to the left side of the sella. There is also the right cavernous sinus involvement.

Intratumoral hemorrhage is very often found in prolactinomas, especially after the treatment with bromocriptine. However, the hemorrhage may be revealed on MR images within adenomas in patients, who have not been treated (Bonneville et al., 2005). The hemorrhage shows the characteristic high intensity signal on T1-weighted images (Fig.13). A "fluid-fluid level" can be seen within the hemorrhage, and this feature is typical and more common in adenomas compared to other tumors, such as craniopharyngiomas.

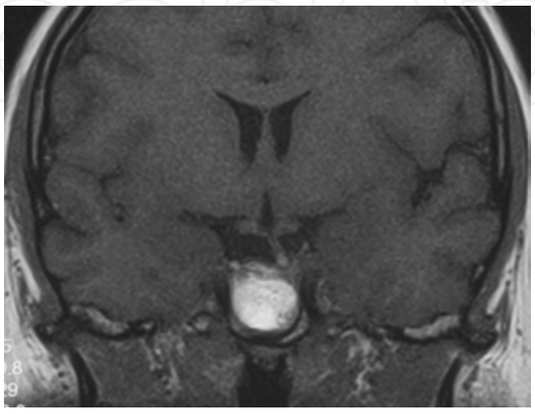


Fig. 13. T1-weighted coronal unenhanced image. The high intensity area of hemorrhage within prolactine-secreting macroadenoma is visible.

Macroadenomas are intrasellar masses usually with extrasellar extension. They may grow upwards causing the optic chiasm compression and indent the floor of the third ventricle. These tumors can also extend downward into the sphenoid sinus, back into the dorsum sellae or laterally into the cavernous sinus. Involvement of the cavernous sinus can modify the prognosis, therefore the correct diagnosis is of high clinical importance, although it may remain difficult to differentiate compression and involvement. The complete encasement of the intracavernous part of the internal carotid artery (ICA) by the adenoma is the best sign of involvement of the cavernous sinus (Fig.14) (Bladowska et al., 2004).

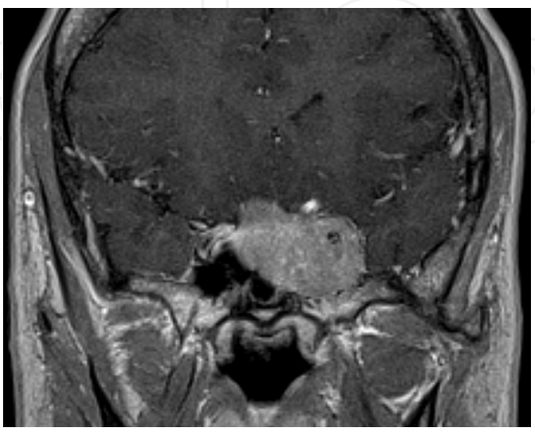


Fig. 14. T1-weighted coronal contrast-enhanced image. The complete encasement of the intracavernous part of the left internal carotid artery by the adenoma is visible.

4. Imaging of other pituitary tumors and parasellar lesions

The most common pituitary tumors are adenomas, the other tumors constitute approximately 5 to 10% of all sellar and parasellar lesions. The precise knowledge of the MR appearance of these lesions is of high importance in clinical practice, because they can mimic pituitary adenomas. In this subsection we describe the characteristic imaging features of these tumors.

4.1 Craniopharyngiomas

Craniopharyngiomas are the most common suprasellar lesions. They account for approximately 3% of all intracranial neoplasms and are slow-growing, benign tumors, which arise from squamous epithelial cell rests of Rathke's pouch. These tumors are frequent in children and young adults, but they also can be found in older adults. Craniopharyngiomas may be divided into two histological types: adamantinomatous and squamous-papillary (Doerfler & Richter, 2008).

In MR imaging the signal intensity of craniopharyngioma varies with cyst contents. High T1 signal is the results of high protein content (Fig.15). The classic adamantinomatous type usually consists of hyperintense cysts and heterogeneous nodules. The less common papillary type is presented with isointense solid component. On T2-weighted images cysts are predominantly hyperintense, while the solid components show heterogeneous signal. After contrast administration the solid portions enhance heterogeneously, as well as cysts walls reveal strong enhancement (Bladowska et al. 2004; Doerfler & Richter, 2008).

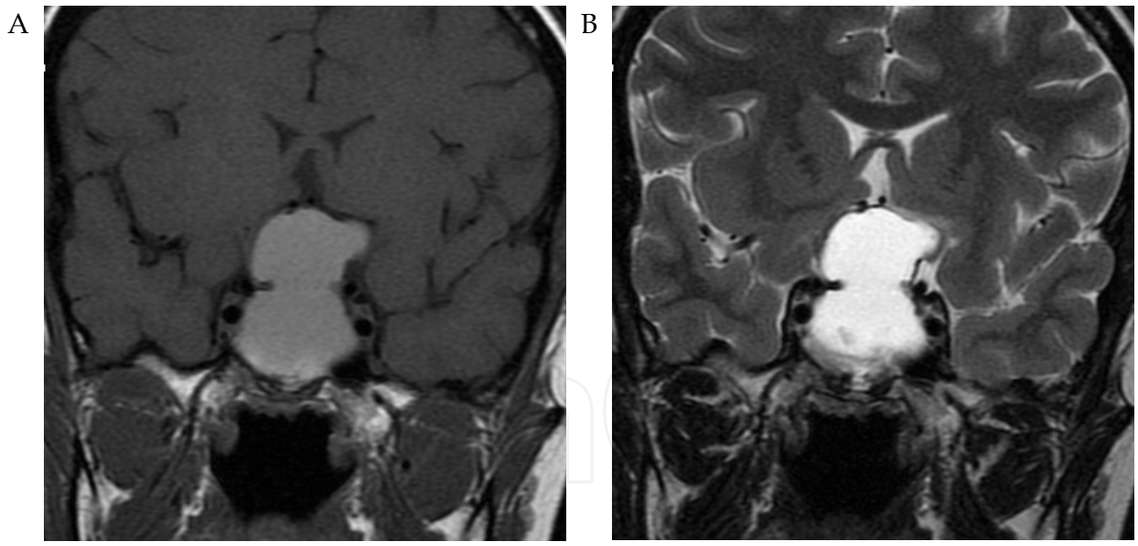


Fig. 15. MR imaging in coronal planes before contrast administration. A. T1-weighted image. B. T2-weighted image. The sellar-suprasellar craniopharyngioma presents with high signal intensity on both T1- and T2-weighted images.

4.2 Rathke's Cleft Cyst

Rathke's cleft cysts account for approximately 1.5% of all sellar and parasellar lesions. They, like craniopharyngiomas, are also derived from the Rathke's pouch, but are usually smaller and almost always located intrasellar, between the anterior and posterior pituitary lobe.

Furthermore, they present with different histological structure compared to craniopharyngiomas - Rathke's cysts are lined by a single layer of epithelium, while craniopharyngiomas have thick walls composed of squamous or basal cells (Bladowska et al. 2004; Doerfler & Richter, 2008).

Rathke's cleft cysts are relatively common incidental findings, usually remaining asymptomatic.

In MR imaging Rathke's cleft cysts display variable signal intensity. Cysts containing serous fluid are typically hypointense on T1-weighted images and hyperintense on T2-weighted images (Fig.16), while mucoid cyst reveal high signal intensity on T1-weighted images and often characteristic very low signal on T2-weighted images (Fig.17). After contrast administration they usually do not enhance, although sometimes they can show very thin rim enhancement.

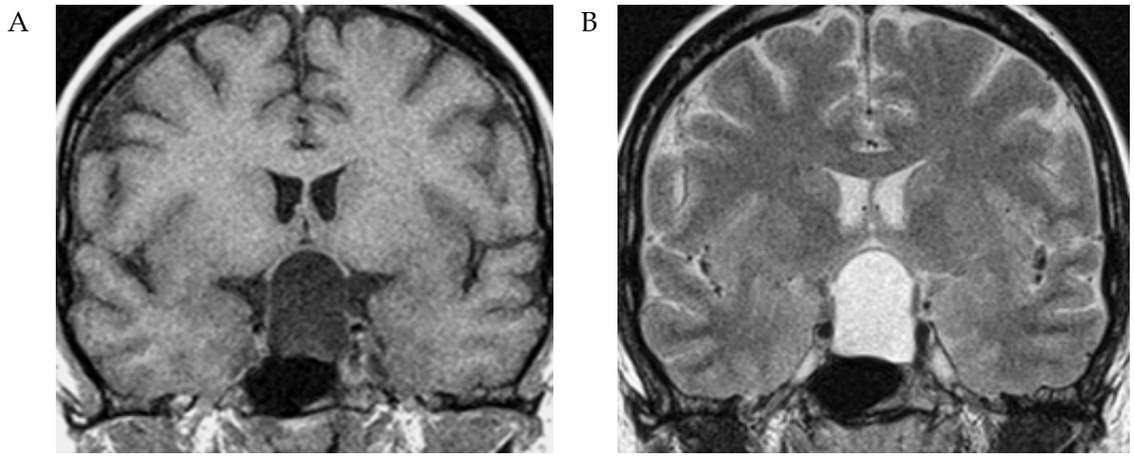


Fig. 16. MR imaging in coronal planes before contrast administration. A. T1-weighted image. B. T2-weighted image. Rathke's cleft cyst containing serous fluid – it is hypointense on T1 and hyperintense on T2-weighted image.

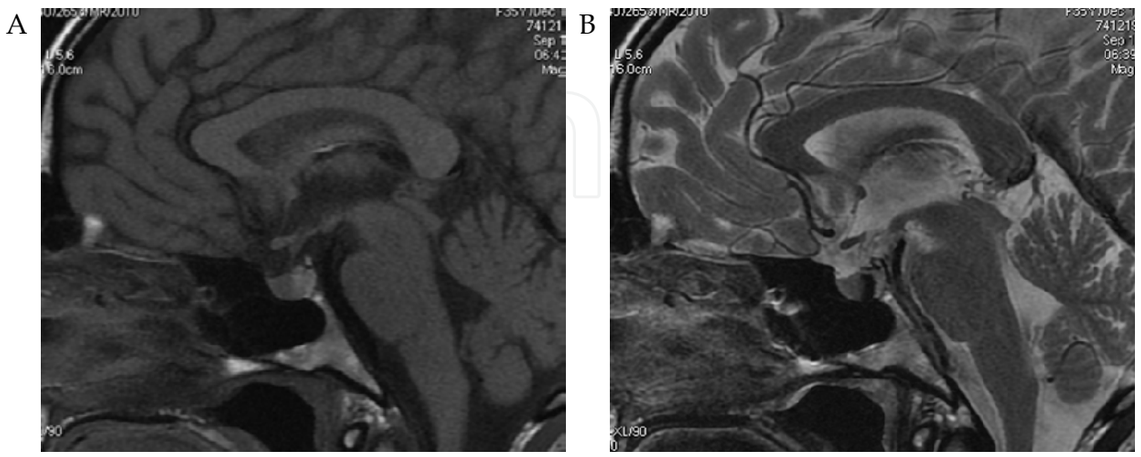


Fig. 17. MR imaging in sagittal planes before contrast administration. A. T1-weighted image. B. T2-weighted image. Rathke's cleft cyst containing mucoid fluid – it is hyperintense on T1 and hypointense on T2-weighted image.

Other cysts located in the sellar and parasellar region include: arachnoid, dermoid, epidermoid and colloid cysts (Bladowska et al., 2010c; Doerfler & Richter 2008).

4.3 Meningiomas

Meningiomas of the sellar region (cavernous sinus, planum sphenoidale, diaphragm sellae and clinoid process) account for about 11% of all sellar and parasellar tumors and for 20-30% of all intracranial meningiomas (Doerfler & Richter 2008). They are slow-growing, usually benign tumors.

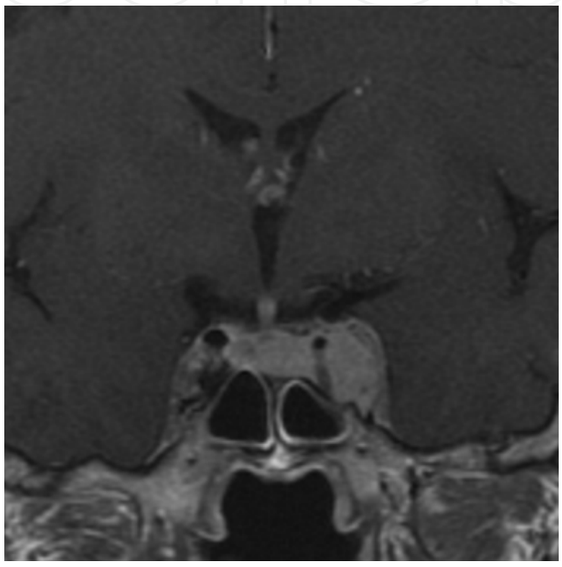


Fig. 18. T1-weighted coronal contrast-enhanced image. The meningioma of the left cavernous sinus is visible.

In MR imaging meningiomas are isointense compared to grey matter on T1-weighted images and isointense or slightly hyperintense on T2-weighted images. After contrast administration they reveal homogeneous enhancement (Fig.18). Often they present with characteristic so-called "dural tail sign", what can help in differential diagnosis, but it has to be stressed that the "dural tail sign" is a nonspecific feature and may also be visible in other intracranial tumors.

4.4 Other rare sellar and parasellar lesions

Rare primary neoplasm of the pituitary and sellar region include: melanoma, intrasellar meningioma, germinoma, choristoma, glioma and metastases (Elster 1993; Ruscalleda 2005). Inflammatory and infectious lesions of pituitary and sellar region include: abscess (Fig.19) (Bladowska et al., 2010d), sarcoidosis, cysticercosis, Langerhans cell histiocytosis, blastomycosis, Wegener granulomatosis, Tolosa-Hunt syndrome, lymphocytic adenohypophysitis, giant cell granuloma and tuberculosis (Elster 1993; Doerfler & Richter 2008).

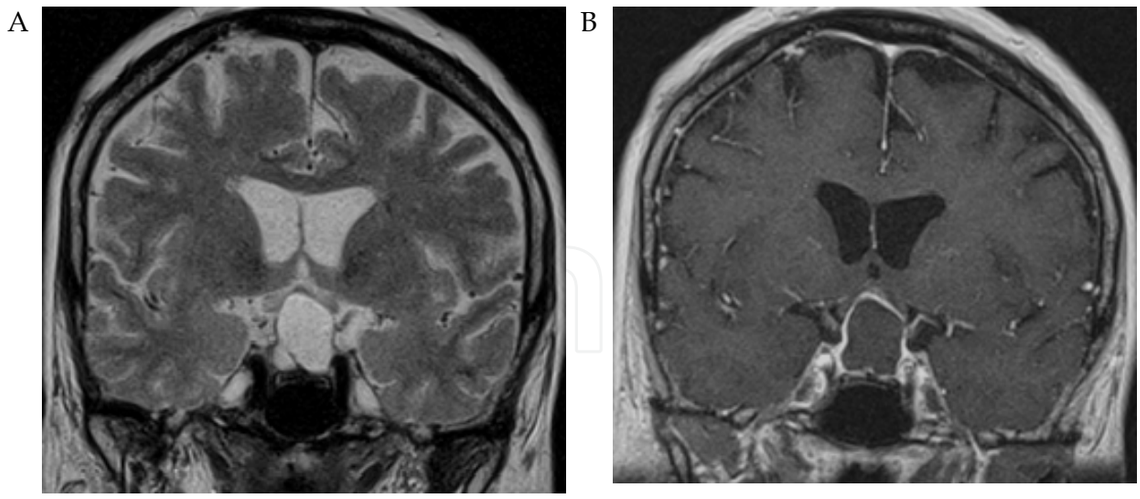


Fig. 19. MR imaging in coronal planes of the pituitary abscess. A. T2-weighted unenhanced image. B. T1-weighted contrast-enhanced image. There is characteristic strong rim enhancement visible.

5. Postoperative MR imaging of pituitary and sellar region – own experience

Post-surgical evaluation of the pituitary gland in MR is difficult because of a change in anatomical conditions. Interpretation of MR images taken after surgical therapy of pituitary tumors depends also on numerous other factors, including: size and expansion of a tumor before operation, type of surgical access, quality and volume of filling material and time of its resorption. Proper evaluation of post-surgical MR images is crucial for determination of completeness of the resection. Therefore neuro-radiologists face a responsible and difficult task of evaluation of structures present in the surgical area, and especially of differentiation of residual tumor from the implanted material and from post-surgical changes (fibrous and cicatrical), or even from a part of normal gland left at site (Bladowska et al., 2010a,b).

In general, the residual tumors could be differentiated from postoperative changes by means of location, characteristic signal intensity and enhancing pattern, which should be similar to those in the preoperative MR imaging of the tumor. The infundibulum tilt could be additional factor suggesting the presence of residual adenoma. The endocrine studies are very helpful in postoperative diagnosis of hormone-secreting residual pituitary adenomas and are regarded as a method of choice in postoperative management of these tumors. It is especially difficult to evaluate the effectiveness of the surgical treatment of the nonfunctioning pituitary tumors, these tumors require a postsurgical MR follow-up examinations.

The basic therapeutic method of pituitary tumors (apart from microprolactinoma) is surgery. Among several operation methods of the sellar region, the most frequently applied is the one with transnasal transsphenoidal approach. This method has widely forced out craniotomy and is now concerned the method of choice in the treatment of the majority of pituitary adenomas, both the hormonally active and inactive ones (Bladowska et al., 2010b).

A characteristic feature of transsphenoidal surgery is the necessity of applying different filling materials to obtain haemostasis, to fill the resection site within the sella, and to inhibit the outflow of the CSF (cerebrospinal fluid).

Filling materials are foreign or autogenic bodies that do not become vascularised. To sustain haemostasis, the following materials are used: oxidized cellulose (Oxycel or Surgicel), spongostan (Gelfoam), tissue glue (Tissucol or Beriplast), bone wax (to restrain bleeding from bone). Liquorrhoea requires a reconstructive operation of sella, with the use of autogenic fascia, lyophilisated dura mater or tissue glue. Next, the sella is sealed with a muscle or flakes of oxidized cellulose. To close the bottom of the sella, it is necessary to use a fragment of the collected cartilaginous septum from the nose, the vomer, or a silicon plate. To protect the postresection site and to reinforce the bottom of the sella, an autogenic fat graft is implanted in the sphenoid sinus. The graft is collected from the fatty tissue of the lateral part of the thigh or from the patient's abdomen (Bladowska et al., 2010b).

Application of the filling materials constitutes a considerable challenge in interpretation of the MR imaging results in patients who underwent surgery of the pituitary tumors. This can also lead to misdiagnosis. The knowledge of MR characteristics of the implanted materials is very important in postoperative diagnosis of pituitary tumors and may help to discriminate between tumorous and non-tumorous involvement of the sellar region (Bladowska et al., 2010b).

In the MRI examination, on T1-weighted images, Surgicel (Oxycel) is represented by a heterogeneous structure with a regular, oval shape, low signal intensity, surrounded by a hyperintense rim. Examinations performed in the first days after the procedure, frequently reveal the presence of small air bubbles closed in the strips of Surgicel, in the hypointense central part of the filling material (Bladowska et al., 2010b; Bonneville et al., 2003).

Spongostan (gelfoam) is represented in the MRI examination by an intrasellar mass of signal intensity similar to that of the grey matter. In rare cases, spongostan may produce a heterogeneous high signal caused most probably by the presence of methemoglobin (Bladowska et al., 2010b; Bonneville et al., 2003).

The similarity between signal intensity of the filling material, of the anterior pituitary lobe, and of a potential residual tumour often makes it difficult to interpret the image in an unequivocal way and to carry out a correct differential diagnosis. However, according to T. Kilic et al., spongostan and Surgicel (Oxycel) may be recognised only on an early performed MRI, i.e. within 24–48 hours after the procedure, because afterwards, the materials begin to undergo a progressive degeneration and their radiological identification becomes harder (Kilic et al., 2001). E. Steiner et al reported that these materials are normally recognisable on MRI for up to 3–6 months after the procedure (Steiner et al., 1992). Our studies showed that haemostatic materials may be identified only in the early postoperative period – in own material is was 1 month (Fig.20) (Bladowska et al., 2010b).

After contrast administration, the central part of the haemostatic material remained hypointense, with peripheral rim of enhancement. This peripheral enhancement is caused by granulation tissue forming around the implanted material. Filling materials undergo changes which surely inhibit their identification. It should be underscored that a hypointense mass with peripheral enhancement after contrast administration is not characteristic for the filling material only. It may also correspond to the presence of a fluid

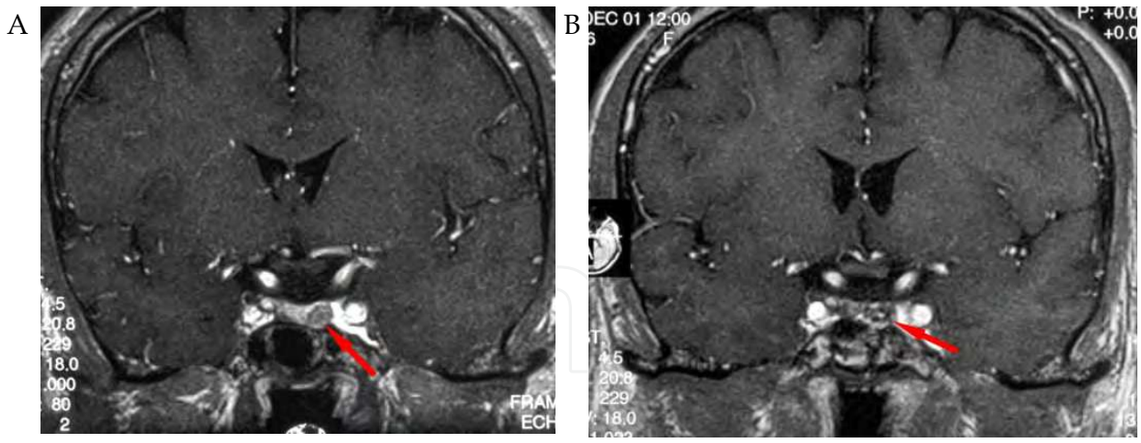


Fig. 20. T1-weighted contrast-enhanced coronal images. A. Before operation – on the left side of the pituitary the microadenoma is visible (arrow). B. Follow-up MRI performed 1 month after surgery – there is haemostatic material implanted into the operation site (arrow).

cistern, regions of necrosis within the tumor or cicatrical fibrous tissue with granulation around it (Bladowska et al., 2010b; Bonneville et al., 2003).

In our own material, as much as 85.61% of the patients had their first postoperative MRI examination performed after 3 months following the procedure, and only 14.39% of the studied individuals (20 patients) – during the first 3 months. There were no examinations carried out within 24–48 hours from the procedure. When we consider the date of MRI examinations and the fast degeneration of the filling material, it is then easy to explain the fact why the haemostatic material was identified in only two patients of the studied group.

The analysis of the conducted examinations revealed that the implanted autogenic fat and muscle with fascia, located in the lumen of the sphenoid sinus, can be observed on MRI for much longer (Bladowska et al., 2010b).

Fatty tissue is not too difficult to identify, as it provides a characteristic signal of high intensity on T1-weighted images (Fig.21). There were reported cases of residual fatty material present in the sphenoidal sinus examined at 1–2 years after the procedure or even 3–4 years afterwards. However, according to our assessments, the implanted fat may remain in place for much longer. The volume of the implanted fat influences the duration of its presence on MRI. Normally, the adipose tissue implanted in larger amounts (in case of macroadenoma resection) retains for much longer than the small amount of that material (implanted after microadenoma resection), absorbed within 9–12 months.

As compared to other filling materials, identification of the fatty tissue in the MRI examination is easy thanks to the characteristic high signal intensity produced by the material, its longer persistence, but also the absence of adjacent contrast-enhanced areas formed by the granulation tissue.

In the studied material, the implanted fatty tissue was identified in as many as 86 patients after pituitary tumour surgery. In the remaining 12 patients, who according to surgical reports were implanted fatty filling material, it was impossible to find that material on MRI. No fatty tissue found in these patients may result from a small amount of the implanted material, from its fast absorption, as well as from a longer postoperative time to MRI examination.

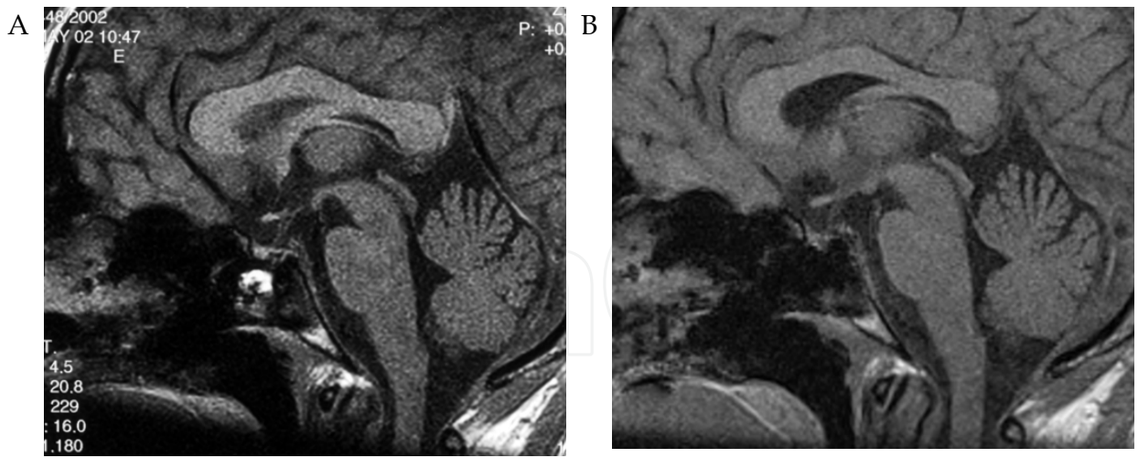


Fig. 21. T1-weighted unenhanced sagittal images. A. MRI performed 10 months after transsphenoidal operation reveals the implanted fatty material inside the sphenoid sinus – it presents with high signal intensity. B. Follow-up MRI performed 23 months after surgery – there is no implanted material visible.

The earliest total absorption of the fatty material was observed 11 months after the procedure. In most of the cases, residues of the adipose tissue were present for a long time, for even up to 112 months (nearly 10 years) after the procedure, while in one patient, there was a large amount of the fatty material still present in the lumen of the sphenoidal sinus after 348 months (29 years) (Bladowska et al., 2010b).

In 2 patients, it was possible to visualise the implanted titanium mesh (Fig.22). On MRI, the titanium mesh was represented by a linear area producing no signal and located in the bottom of the sella (Bladowska et al., 2010b).

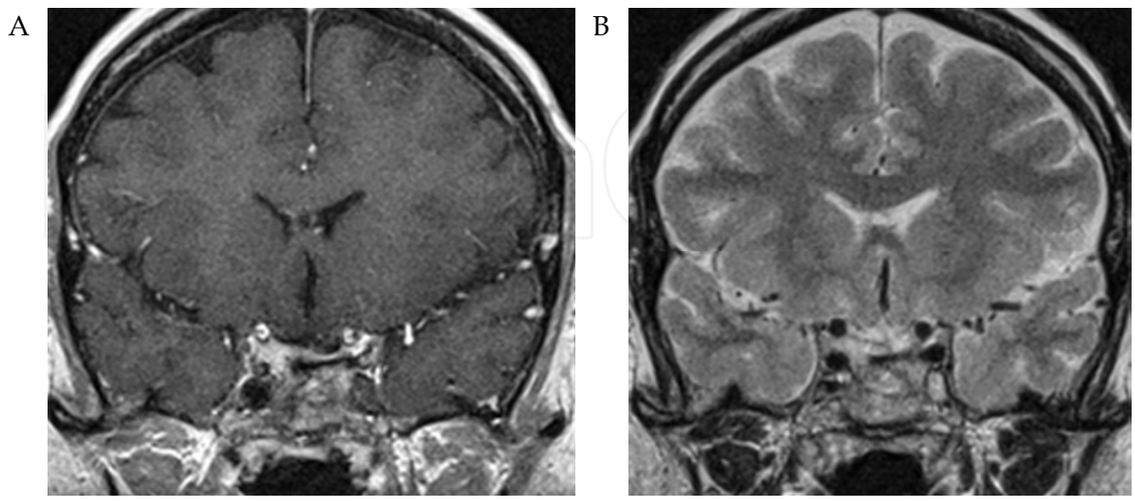


Fig. 22. MR imaging of implanted titanium mesh. A. T1-weighted coronal image. B. T2-weighted coronal image. A linear area producing no signal and located in the bottom of the sella is visible.

In 3 individuals, an implanted muscle with fascia was identified. It was represented by a round, isointense structure, filling nearly the whole sphenoidal sinus on T1-weighted MRI images. After intravenous contrast administration, the structure was becoming slightly enhanced in its peripheral part, with a central round area of lower signal intensity (Fig.23a). Such an image of the implanted muscle was found in 2 patients after 4 months following the procedure, and in 1 patient after 5 months from surgery. The follow-up MRIs (beginning approx. from the 12th postoperative month) were revealing a gradual change in the image of that material. After contrast administration, the previously distinct border between the enhanced peripheral part and the central hypointense part of the implanted muscle became indistinct. In further MRI examinations, performed approx. 25 months after surgery or later, the structure present in the lumen of the sphenoidal sinus remained hypointense after contrast administration. Without the analysis of previous images and the knowledge of patient's history, the correct diagnosis of that mass on T1-weighted images was impossible (especially its differentiation from e.g. fluid cistern). The implanted muscle with fascia produced a very characteristic and almost stable image in T2-weighted sequence (Fig.23b), for at least 31 months following the procedure. In the T2-weighted sequence, the material is represented by a hyperintense mass with a linear structure, of a very low signal intensity, corresponding to fascia (Fig.23b). It should also be pointed out that fascia was not identified on T1-weighted images (Fig.23a) (Bladowska et al., 2010b, 2011).

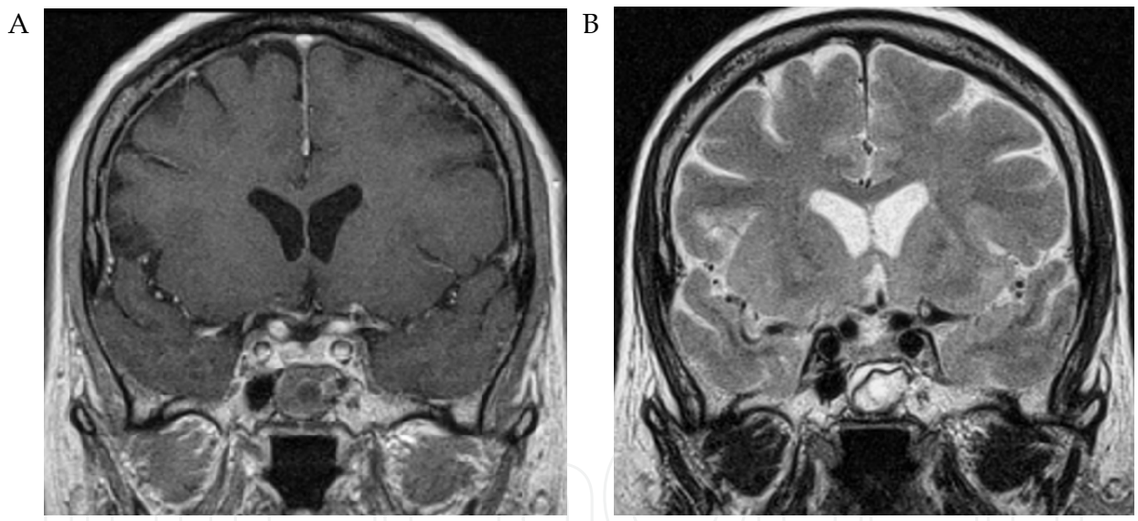


Fig. 23. MR imaging of muscle with fascia implanted into the sphenoid sinus. A. T1-weighted enhanced coronal image. B. T2- weighted unenhanced coronal image – the linear structure, of a very low signal intensity, corresponding to fascia is very well visible.

The final diagnosis and evaluation of the surgical completeness on the basis of the performed MRI is often equivocal, in spite of the presence of the above mentioned criteria.

It is especially hard to evaluate the effectiveness of the surgical treatment of the hormonally inactive tumors on the basis of the MRI examination results and their interpretation only. These tumors require a postsurgical endocrinological and MRI follow-up.

Follow-up of abnormal structures present in the postsurgical area may allow for their verification. If in the following examinations there is a complete absorption of the focal

lesion, this excludes the presence of a residual tumor and indicates to the filling material or postoperative changes.

If the size and volume of the pathological structure increases, this points to the presence of a residual tumor. On the other hand, it should be remembered that pituitary tumors grow slowly, so in a long-term follow-up, the tumor may seem stable, which does not facilitate the final diagnosis in unclear cases of hormonally inactive tumors.

As mentioned above, the transsphenoidal approach is currently the method of choice in treatment of most of pituitary tumors. There are characteristic changes inside the sphenoid sinus after the surgery (Connor & Deasy, 2002). MRI findings of sphenoid sinus filling (opacification) are present in approximately 37% of examinations performed more than 12 months after transsphenoidal surgery. The contrast enhancement at the margins of the sphenoid sinus, called as Rodriguez's changes (Fig.24), is always apparent in cases of hypervascularized and swollen mucosa (Rodriguez et al., 1996) and could persist even 10 years after surgery.

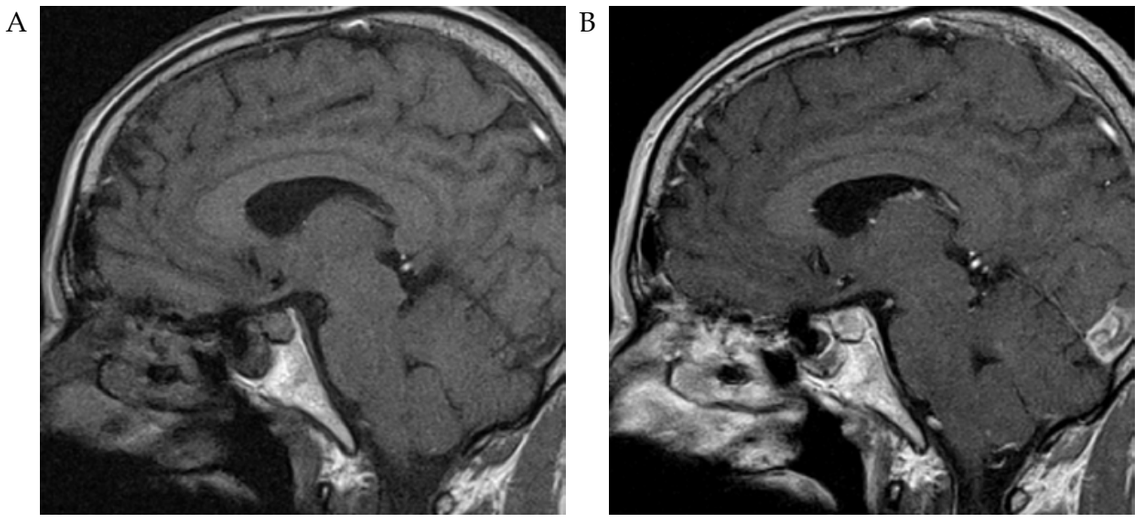


Fig. 24. MR imaging of Rodriguez's changes, T1-weighted sagittal images: unenhanced (A), contrast-enhanced (B). There are hypointense masses inside the sphenoid sinus, which show the characteristic rim contrast enhancement.

The special attention should be also paid to usefulness of T2-weighted images in assessment of postoperative sella and sellar region. T2-weighted images may help to discriminate between tumorous and non-tumorous involvement of the postoperative sella and the sphenoid sinus especially in cases, in which the signal intensity and enhancement pattern of pituitary gland and tumor are the same on T1-weighted images. T2-weighted images are also very useful in the postoperative evaluation of the implanted muscle with fascia, especially during long term follow-up. The best protocol for the postoperative imaging after pituitary tumor resections should include both T1- and T2-weighted imaging, because T1- and T2-weighted images supplement each other in the postoperative examination of the sella and sellar region. However, in some cases T2 could replace post-contrast T1, especially in patients with high risk of Nephrogenic Systemic Fibrosis (NSF) (Bladowska et al., 2011).

6. Conclusion

Pituitary adenomas are common neoplasm, they account for 10-15% of all diagnosed intracranial tumors. The proper diagnosis and management of patients with pituitary lesions are of high importance in the clinical practice. Currently, MR is the method of choice for imaging of the pituitary gland and the parasellar area. MR imaging protocol of pituitary and sellar region including postoperative studies should consist of unenhanced T1- and T2-weighted images in coronal and sagittal planes, followed by T1-weighted images after contrast administration. Because of so many pathological changes with different clinical and radiological appearances of the lesions located in sellar and parasellar region, the precise knowledge of pituitary lesions is mandatory for the correct diagnosis and management of patients with pituitary diseases.

7. Acknowledgment

I would like to thank my dear husband Maciej, my lovely daughters Justynka and Hania, and my all family for the patience, they have given me during the time I was writing this chapter. I will use the words of Robert C. Martin:

"There is no greater treasure, nor any wealthier trove, than the company of my family, and the comfort of their love".

Joanna Bladowska

8. References

Arslan A., Karaarslan E., Dincer A. (1999) High intensity signal of the posterior pituitary. A study with horizontal direction of frequency-encoding and fat suppression MR techniques. *Acta Radiologica*, Vol. 40, (1999) pp. 142-145.

Bladowska J., Sokolska V., Czapiga E., Badowski R., Koźmińska U., Moroń K. (2004) Advances in diagnostics imaging of the pituitary and the parasellar region. *Advances in Clinical and Experimental Medicine*, Vol. 13, (2004) pp. 709-717.

Bladowska J, Sokolska V, Sozański T et al. (2010) Comparison of post-surgical MRI presentation of the pituitary gland and its hormonal function. *Polish Journal of Radiology*, Vol. 75, (2010) pp. 29-36.

Bladowska J, Bednarek-Tupikowska G, Sokolska V et al. (2010) MRI image characteristics of materials implanted at sellar region after transsphenoidal resection of pituitary tumours. *Polish Journal of Radiology*, Vol.75, (2010), pp. 46-54.

Bladowska J, Bednarek-Tupikowska G, Biel A, Sąsiadek M. (2010) Colloid cyst of the pituitary gland: Case report and literature review. *Polish Journal of Radiology*, Vol.75, (2010), pp. 92-97.

Bladowska J, Bednarek-Tupikowska G, Sokolska V, Czapiga E, Czapiga B, Sąsiadek M. (2010) Unusual presentation of recurrent pituitary abscess – a case report and literature review. *Neuroradiology Journal*, Vol.23, (2010), pp. 547-553.

Bladowska J, Biel A, Zimny A et al. (2011) Are the T2-weighted images more useful than T1-weighted contrast-enhanced images in assessment of postoperative sella and parasellar region? *Medical Science Monitor*, Vol. 17, no 10 (October 2011), pp. MT83-MT90.

Bonneville JF. (2000) Pituitary adenomas: value of MR imaging. *Journal of Radiology,* Vol.81, (2000), pp. 939-942.

Bonneville JF, Bonneville F, Schillo F, Cattin F, Jacquet G. (2003) Follow-up MRI after trans-sphenoidal surgery. *Journal of Neuroradiology,* Vol.30, (2003), pp. 268-279.

Bonneville JF, Bonneville F, Cattin F. (2005) Magnetic resonance imaging of pituitary adenomas. *European Radiology*, Vol. 15, (2005) pp. 543-548.

Boxerman JL, Rogg JM, Donahue JE et al. (2010) Preoperative MRI evaluation of pituitary macroadenoma: imaging features predictive of successful transsphenoidal surgery. *American Journal of Radiology AJR,* Vol.195, (2010), pp. 720-728.

Chernov MF., Kawamata T., Amano K. et al. (2009) Possible role of single-voxel ^{1}H-MRS in differential diagnosis of suprasellar tumors. *Journal of Neurooncology,* Vol.91, (2009), pp. 191-198.

Connor SEJ. & Deasy NP. (2002) MRI appearances of the sphenoid sinus at the late follow-up of trans-sphenoidal surgery for pituitary macroadenoma. *Australasian Radiology*, Vol.46, (2002), pp. 33-40.

Daly AF, Tichomirowa MA, Beckers A. (2009) The epidemiology and genetics of pituitary adenomas. *Best Practice & Research Clinical Endocrinology & Metabolism*; Vol.23, (2009), pp. 543–554.

Doerfler A. & Richter G. (2008) Lesions within and around the pituitary. *Clinical Neuroradiology*; Vol.18, (2008), pp. 5-18.

Elster A.D. (1993) Modern imaging of the pituitary. *Radiology,* Vol.187, (1993), pp. 1-14.

Elster A.D., Chen M.Y.M., Williams D.W., Key L.L. (1990) Pituitary gland: MR imaging of physiologic hypertrophy in adolescence. *Radiology,* Vol.174, (1990), pp. 681-685.

Elster A.D., Sanders T.G., Vines F.S., Chen M.Y.M. (1991) Size and shape of the pituitary gland during pregnancy and post partum: measurement with MR imaging. *Radiology*, Vol.181, (1991), pp. 531-535.

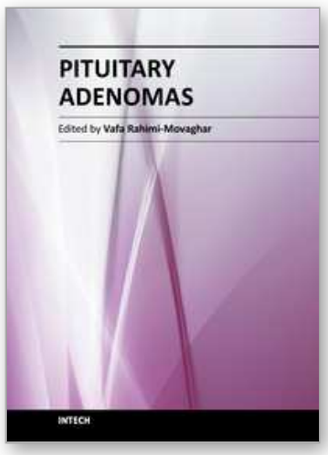
Evanson J. (2002) Imaging the pituitary gland. *Imaging*, Vol.14, (2002), pp. 93-102.

Kilic T, Ekinci G, Seker A et al. (2001). Determining optimal MRI follow-up after transsphenoidal surgery for pituitary adenomas: scan at 24 hours postsurgery provides reliable information. *Acta Neurochirurgica* (Wien), Vol.143, (2001), pp. 1103–26.

Rodriguez O, Mateos B, de la Pedraja R et al. (1996) Postoperative follow-up of pituitary adenomas after transsphenoidal resection: MRI and clinical correlation. *Neuroradiology*, Vol.38, (1996), pp. 747–54.

Ruscalleda J. (2005) Imaging of parasellar lesions. *European Radiology*, Vol.15, (2005), pp. 549-559.

Steiner E, Knosp E, Herold ChJ et al (1992): Pituitary adenomas: Findings of postoperative MR imaging. *Radiology*, Vol.185, (1992), pp. 521–27.



Pituitary Adenomas

Edited by Prof. Vafa Rahimi-Movaghar

ISBN 978-953-51-0041-6
Hard cover, 86 pages
Publisher InTech
Published online 10, February, 2012
Published in print edition February, 2012

Pituitary Adenomas is a comprehensive book about the most common pathology of the pituitary gland in the sellar region. The book chapters include epidemiology, symptoms and signs, clinical, imaging, immunohistochemical and ultrastructural pathological diagnosis, therapeutic approaches and outcome of the functional and non-functional pituitary tumors. Therapies include medications, endoscopic transphenoidal and open surgeries; radiotherapy includes gamma knife radiosurgery. Visual symptoms has important and characteristic patterns which has discussed in one specific chapter. Endocrine secretion is another characteristic in 40% of pituitary adenomas. Therefore, another chapter presents it. Stereotactic radiosurgery and endoscopic surgery both have special role in recent decades. Thus, they have considered specifically, too. Authors expect to give excellent insight in pituitary adenoma to the book readers.

How to reference

In order to correctly reference this scholarly work, feel free to copy and paste the following:

Joanna Bladowska and Marek Sąsiadek (2012). Diagnostic Imaging of the Pituitary and Parasellar Region, Pituitary Adenomas, Prof. Vafa Rahimi-Movaghar (Ed.), ISBN: 978-953-51-0041-6, InTech, Available from: http://www.intechopen.com/books/pituitary-adenomas/diagnostic-imaging-of-the-pituitary-and-parasellar-region

INTECH
open science | open minds

InTech Europe
University Campus STeP Ri
Slavka Krautzeka 83/A
51000 Rijeka, Croatia
Phone: +385 (51) 770 447
Fax: +385 (51) 686 166
www.intechopen.com

InTech China
Unit 405, Office Block, Hotel Equatorial Shanghai
No.65, Yan An Road (West), Shanghai, 200040, China
中国上海市延安西路65号上海国际贵都大饭店办公楼405单元
Phone: +86-21-62489820
Fax: +86-21-62489821

© 2012 The Author(s). Licensee IntechOpen. This is an open access article distributed under the terms of the Creative Commons Attribution 3.0 License, which permits unrestricted use, distribution, and reproduction in any medium, provided the original work is properly cited.

IntechOpen

IntechOpen